Construction and Building Materials 23 (2009) 2518–2526

Contents lists available at ScienceDirect

Construction and Building Materials

journal homepage: www.elsevier.com/locate/conbuildmat

Combined effect of two sustainable technologies: Self-compacting concrete (SCC) and controlled permeability formwork (CPF)

Helena Figueiras, Sandra Nunes, Joana Sousa Coutinho *, Joaquim Figueiras

LABEST – Laboratory for Concrete Technology and Structural Behaviour, Department of Civil Engineering, Faculty of Engineering, University of Porto, Rua do Dr. Roberto Frias s/n, 4200-465 Porto, Portugal

ARTICLE INFO

Article history:
Received 7 July 2008
Received in revised form 26 December 2008
Accepted 8 February 2009
Available online 5 April 2009

Keywords:
Durability
Sustainable technology
Self-compacting concrete
Controlled permeability formwork
Mechanical and durability properties

ABSTRACT

The work presented in this paper aims at contributing to sustainable construction through enhancement of durability of concrete structures. Full size precast elements were cast with both self-compacting concrete (SCC) and conventional vibrated concrete (CC) using controlled permeability formwork (CPF). SCC is known to impart a more homogeneous and finer microstructure, compared to conventional concrete, therefore leading to more durable reinforced and pre-stressed concrete structures. CPF enables, in fresh concrete, drainage of excess water and air besides retaining binder particles at the concrete surface, leading to a blow-hole free surface and enhanced quality of the outer layers. The research program developed was designed to compare performance of two different CPF systems and also assess the combined effect of using CPF on SCC compared to CC.

1. Introduction

It is needless to say that concrete has played an extremely important role in the construction of various structures for the improvement of our living environment. An enormous amount of concrete has been used as a construction material. There is no doubt that its use as a major construction material will continue in the future [1]. Concrete for the 21st century will have to be more durable, easier to apply, more predictable and greener. At the same time it will have to be more cost competitive [2]. In fact there is extensive evidence to show that concrete materials and concrete structures all over the world are deteriorating at a rapid rate, and that it has not been possible to ensure their long-term durable service life performance. A durable, efficient and effective infrastructure system is fundamental to economic prosperity, social justice, political stability and the quality of human life. However, sustainability in construction cannot be achieved if used materials and built structures cannot give durable service life. In fact, material degradation and structural damage in service shows that the progress of damage involves many interactive and interdependent parameters, several of which are beyond the control of engineers, and indeed, not anticipated or fully appreciated at the design stage. The complex, highly unpredictable and extremely variable interactive effects of load, ageing, cracking, exposure conditions and climatic changes emphasize the limitations of what is understood of the performance of materials and structures in real life exposure conditions. Therefore to achieve durable service life performance, a holistic durability design philosophy must be used, this is, an integrated material and structural design strategy of strength through durability rather than of durability through strength, where materials are manufactured for durability rather than for strength, and structures are designed for ductility and structural integrity. Holistic design envisages a global approach to all aspects of concrete and construction technology from material selection, design, construction, and maintenance to service life, integrating material characteristics with *in situ* performance [3].

In particular, durability of concrete structures depends primarily on permeability of the outer concrete cover which, generally, is a result of the production standard, casting conditions, compaction in heavily reinforced areas and curing conditions. The growing need to achieve durable service life performance may require considering additional protective measures which hinder corrosion and concrete degradation. In fact, using controlled permeability formwork (CPF) or self-compacting concrete (SCC) enhance quality of the concrete cover and therefore resistance to ingress of aggressive agents.

SCC, initially developed in Japan [4], consists of a social, economical and environmental sustainable technology. SCC probably corresponds to the most revolutionary step of the last decades, in terms of concrete technology. It involves a new production and casting process in where compaction is banned. This leads to reduction in casting costs and a more homogeneous product [4–6]. In fact, SCC compared to conventional concrete (CC) is free of local variation due to man-dependent poker vibration. Also, as SCC

* Corresponding author. Tel.: +351 225081936; fax: +351 225081446.
E-mail address: jcouti@fe.up.pt (J.S. Coutinho).

0950-0618/$ - see front matter © 2009 Elsevier Ltd. All rights reserved.
doi:10.1016/j.conbuildmat.2009.02.035

uses more powdered materials than CC, imposed by fresh-state properties, this potentially leads to better durability performance. Using mineral additions finer than cement, enables hydration to a denser matrix, less permeable to aggressive agents, therefore postponing and hindering deterioration.

Controlled permeability formwork (CPF) is one of the few techniques for directly improving the concrete surface zone. This technique reduces the near surface water/binder ratio and reduces the sensitivity of the concrete to poor site curing. CPF consists of using a textile liner on usual formwork, allowing air bubbles and surplus water to drain out but retaining binder particles and so enabling the water-binder ratio of the outer layer to become very low and the concrete to hydrate to a very dense surface skin as the filter makes enough water available at the right time to activate optimum hydration. So CPF enhances durability by providing an outer concrete layer which is richer in binder particles, with a lower water/binder ratio, less porous and so much less permeable than when ordinary formwork is used [7]. Although CPF has proved to improve the quality of the concrete cover, it does not prevent CC problems resulting from poor compaction or aggregate nesting induced by lack of paste.

Considering the advantages and limitations of both additional protective measures, SCC and CPF, it is possible that they will reveal a synergetic effect, thus further enhancing durability performance of concrete structures. Therefore the aim of this work is to assess the efficiency of two CPF systems on SCC and on conventional concrete (CC) and compare the effect of each of the systems used. Two box-culverts, one with SCC and the other with CC were both cast using the two different CPF systems. Mechanical and durability-related properties were compared for the CPF systems and for the box-culverts made of the different types of concrete thus enabling considerations on homogeneity of concrete throughout each element. In the particular case of assessing resistance of concrete to chloride penetration, two different tests were used, the CTH Rapid Method and the ASTM C1202 method. Therefore an analysis comparing test results of both methods is presented.

2. Experimental program

2.1. Materials

Concrete was produced using Portland cement (CEM I 52.5 R) and a mineral addition (limestone filler), of specific gravity 3.12 and 2.70, respectively. The specific surface (Blaine) and the mean particle size of limestone filler were 5150 cm^2/g and 4.52 μm, respectively. A polycarboxylate type superplasticizer of specific gravity of 1.05% and 18.5% solid content was used.

Crushed calcareous aggregate (1–12.5 mm), siliceous natural fine sand (sand 1) with a fineness modulus of 2.52 (ASTM) and a natural coarse sand (sand 2) with a fineness modulus of 3.27 were used, see Table 1. The specific gravity of the coarse aggregate, sand 1 and sand 2 were 2.61, 2.60 and 2.62, and absorption values 1.29%, 0.68% and 0.51%, respectively, according to EN 1097-6 [8].

2.2. Self-compacting concrete mix-design

A key phase when producing SCC lies on the design of mix proportions so as to obtain adequate properties of fresh concrete. SCC in the fresh state must show filling ability, resistance to segregation and passing ability. To achieve these properties, the paste content (including mineral additions and the superplasticizer dosage) has to be increased and the coarse aggregate content must be reduced [6]. The "excess paste" should be the minimal quantity to create a "lubricating" layer around the aggregate particles and reduce the inter-particle friction necessary to achieve self-compactability [9]. Based on the Japanese SCC-designing method, the mix-design method used consisted on a two level (mortar and concrete) optimization method and is described more in detail in [10,11]. At mortar level, mortar flow and funnel tests [10,11] were carried out to study the relation between the two sands (fine aggregate was a combination of two sands) along with paste volume and volumetric water/powder ratio. The mortar properties adequate for SCC are sufficiently well defined at this level [10,11] and if target values are achieved, in the next stage, tests on concrete, although essential, are reduced to a minimum. Final trials at concrete level were necessary to quantify the amount of coarse aggregate, to adjust superplasticizer dosage (if necessary) and to confirm self-compactability of the designed concrete [10,11]. Slump-flow, V-funnel and Box tests were used to characterize SCC in the fresh state. The Slump-flow test is used to evaluate deformation capacity, viscosity and also resistance to segregation of SCC by visual observation. This test enabled recording final slump flow diameter (D_{flow}) and time necessary for concrete to reach a 50 cm diameter (T_{50}). The V-funnel test is used to assess viscosity and passing ability of SCC and this test enabled recording flow time (T_{funnel}). With the Box test it is possible to assess ability of concrete to pass through tight openings between reinforcing bars and filling ability. This test enabled recording filling height (H). Details of the equipment used for testing fresh concrete and test procedures used can be found in [6].

Results concerning fresh SCC testing were D_{flow} = 565 mm, T_{50} = 5.6 s, T_{funnel} = 14.9 s and H = 340 mm. The mixture exhibited good filling ability, high segregation resistance and enough deformability for this type of application. SCC filled up the entire mould, completely enclosing the reinforcement. After stripping the formwork only a few air bubbles were visible on the horizontal parts. The main differences between mix proportions of the SCC and CC, which concern in less coarse aggregate and more powder materials and superplasticizer, can be observed in Table 2. The CC mix corresponded to the one being used at the pre-fabrication plant at the time. It should be noted that the SCC composition was designed to have similar strength the CC composition, at 28 days age.

As both concrete types are clearly different, both in terms of mix proportions and in terms of casting procedures, it is important to analyse and compare hardened properties for each one [12]. Results concerning comparison and evaluation of hardened concrete properties of both, self-compacting concrete and conventional concrete, were presented in Nunes et al. [13].

The differences between mix proportions of SCC and conventional concrete, in terms of coarse aggregate, powder materials and superplasticizer led to an overcost of 18% for SCC. According to Juvas [14] although materials for SCC are 15–25% more expensive than those of normal concrete of the same strength grade, the total costs will be 5–15% lower when all savings in work are included. The difference in costs of materials referred to, will be smaller, the higher the strength class. Therefore, the biggest economic benefits of using SCC correspond to higher grade concrete.

2.3. Controlled permeability formwork systems

Controlled permeability formwork (CPF) consists of using a textile liner on usual formwork, allowing air bubbles and surplus water to drain out but retaining binder particles at the surface of concrete, thus reducing permeability of the outer layer, Fig. 1. CPF also enables the concrete surface to hydrate to a very dense surface skin as the filter makes enough water available at the right time to activate optimum hydration. Besides a blow-hole free surface and an enhanced quality cover concrete, that is durability, due to controlled reduction of the water/binder ratio, CPF reduces pressure on the formwork [15]. An increased volume of a more impermeable and denser paste together with a reduction of the water/binder ratio at the concrete surface may lead to further reduced carbonation and chloride ion ingress as well as a higher resistance to freeze–thaw attack.

One of the aims of this experimental program is to compare performance of two CPF systems, from this point on named CPF-A and CPF-B. These systems were used on two elements, one cast with conventional concrete (CC) and the other with self-compacting concrete (SCC). CPF-A, classified as a Type II system according to the CIRIA Report [16], consists of a single-layer fabric system that is placed over a structural support and tensioned in situ. These systems are usually single-use products. As the fabric is not stiff, tensioning over the mould must be carried out during application to ensure no creases will form, leading to unsightly defects of the concrete surface. CPF-B is a Type III system consisting of a two-layer system combining a filter fabric bonded to a backing grid. This type does not need tensioning. The filter fabric is pre-tensioned in the manufacturing process and tension is maintained by the backing grid. This type may be used more than once. Properties of both CPF systems are shown in Table 3 and Fig. 2 shows CPF applications.

Current cost for CPF-A filter-drain is about 5.00 €/m^2 and 10.00 €/m^2 for CPF-B. The CPF-B filter/drain may be reused once or twice, therefore reducing overall cost. The application cost depends, not only on the system used, but also on the shape of the element. Anyway, the final application cost corresponds to the cost of the filter/

Table 1
Grading of aggregates.

Sieve size (mm)	0.074	0.150	0.297	0.59	1.18	2.38	4.75	6.30	9.5	12.5
Sand 1	1.0	6.7	19.4	44.9	78.0	99.0	100	100	100	100
Sand 2	0.7	3.3	10.1	27.7	53.0	79.5	99.7	100	100	100
Coarse aggregate	0.0	0.11	0.3	0.3	0.3	0.4	6.2	32.4	84.2	100

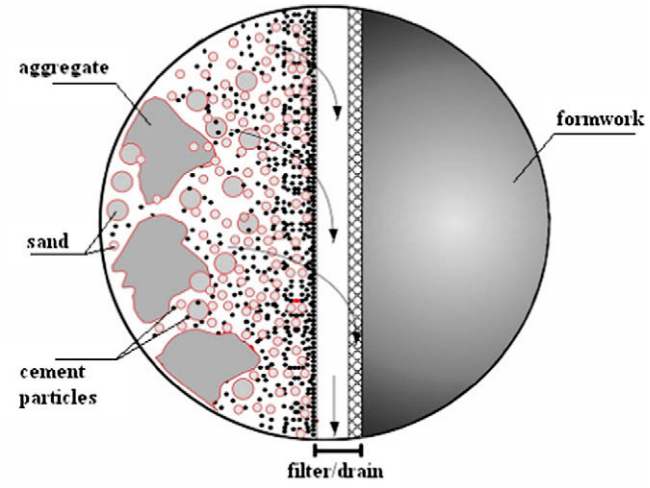

Fig. 1. Schematical representation of CPF functioning.

Table 2
Mix proportions of SCC and conventional concrete produced during full-scale tests.

Constituent materials	SCC (kg/m^3)	CC (kg/m^3)
Cement	387	350
Limestone filler	197	85
Sand 1	618	407
Sand 2	202	413
Coarse aggregate	829	938
Water	138	171
Superplasticizer (liquid)	12.45	3.70[a]
Water/cement (w/c)[b]	0.38	0.49
Water/binder (w/b)	0.25	0.40

[a] Different superplasticizer was used for conventional concrete.
[b] Including water in superplasticizer.

Table 3
Properties of CPF-A and CPF-B filter-drains.

Properties	CPF-A	CPF-B
Composition	100% polypropylene	100% polypropylene
Thickness	1.2 mm	2.0 mm (±10%)
Pore size	<30 μm	<35 μm
Air permeability	0.1–0.5 m^3/m^2 s	<3 m^3/m^2 s

drain plus the application cost but two costs must be deduced: the cost related to the usual concrete surface repairs after stripping common formwork and the cost concerning releasing agent which must not be used with CPF.

Fig. 3. Box-culvert and location of test cores in side wall A.

2.4. Selected elements

The precast concrete elements considered for this research were two identical shaped box-culverts (length = 2.5 m; height = 1.15 m; width = 2.32 m; wall thickness = 0.14–0.16 m, slab thickness = 0.15 m). The box-culverts were cast, as mentioned before, one with SCC and the other with conventional concrete (CC). Each side wall of both box-culverts, SCC and CC, were cast with two different CPF systems, CPF-A and CPF-B. To enable drilling cores from the box-culvert for further testing, three zones with no reinforcement were planned, one in the centre of each side wall and the third on the slab, as shown in Fig. 3. These cores enabled assessment of concrete properties including the effect of both CPF systems considered.

3. Final product

Both box-culverts presented dense concrete with blow-hole free CPF faces standing out against the traditionally cast faces with the usual blow-holes and imperfections which result from air and water retained at the formwork surface during production. Faces showing these blemishes corresponded to the inner facades of both box-culverts and they were more profuse in the CC box-culvert, compared to the SCC one, Fig. 4. The CPF faces, though, had an inconsistent appearance with lighter coloured areas (Figs. 5 and 6) which may have been due to a non uniform concentration of calcareous filler throughout the CPF cast surface. This did not occur at the traditionally cast surfaces.

4. Hardened properties

4.1. Mechanical properties

4.1.1. Specific gravity and compressive strength

Compressive strength of concrete was determined at 60 days on test-specimens cored from the top slab and side walls of each box-culvert. The test-specimens were 94 mm diameter and the height/diameter (h/d) ratio between 1.58 and 1.72. The

Fig. 2. Application of filter-drain A (CPF-A) and filter-drain B (CPF-B) on box-culverts outer side walls A and B.

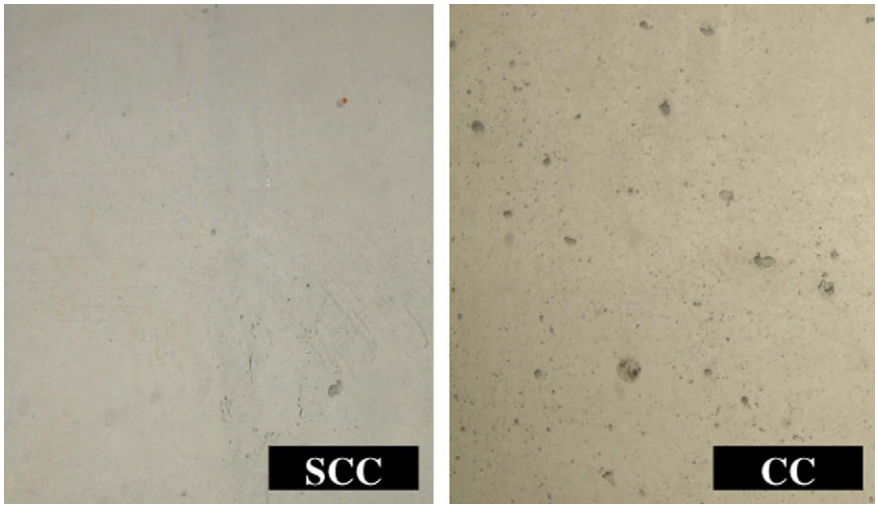

Fig. 4. Detail of concrete surfaces resulting from SCC and CC.

Fig. 5. Concrete surfaces resulting from application of CPF-A on CC box-culvert.

Fig. 6. Concrete surfaces resulting from application of CPF-B on CC box-culvert.

test-specimens from the side walls were loaded perpendicular to casting direction whereas the slab test-specimens were loaded in the same direction. Strength obtained for the test-specimens was converted to values of standard cylindrical test-specimens ($d = 150$; $h = 300$ mm) through relations established by Mansur et al. [17], applicable to strength from 20 to 100 MPa. Converted average strength, specific gravity of concrete and corresponding variation coefficient, from each box-culvert, are presented in Table 4.

SCC strength and specific gravity are similar in the areas analysed along the box-culvert but in the CC box-culvert, values corresponding to the slab are significantly lower compared the side walls, due to lack of efficient compaction in the upper part of the mould. External mould vibration, the usual procedure used for the CC box-culvert, led to uneven and heterogeneous compaction on the upper slab. The effect of this inefficient compaction procedure, in conventional concrete, may produce segregated material with aggregate nesting and, therefore, disclosing varying mechanical and durability properties. As a consequence, in the SCC box-culvert, concrete revealed to be a more homogeneous and isotropic material.

4.1.2. Surface hardness

The most used non-destructive test to estimate concrete strength is the hardness test using a portable Schmidt Hammer. This test assesses the uniformity of the concrete surface layers and also determines hardness which can be correlated to concrete strength. Schmidt Hammer tests following the procedure in EN 12504-2 [18] were carried out on three areas (0.15×0.15 m), at mid-level of the 8 faces of the side walls of the two box-culverts (SCC and CC), at 7, 14 and 28 days. Therefore assessment of the surface hardness was performed on each box-culvert for each side wall: on side wall A, on the outside face corresponding to the CPF-A surface and on the inside face corresponding to the control face, this is, the traditionally cast face; on side wall B, on the outside face corresponding to the CPF-B surface and on the inside face corresponding to the non-CPF face. Results for the SCC and CC box-culvert are shown in Table 5. Values presented include the median, average and variation coefficient for 7, 14 and 28 days of the Schmidt Hammer readings. The graph presented in Fig. 7 shows efficiency of SCC technology and CPF against conventional concrete in accordance with following equation:

$$\text{Efficiency } (\%) = \frac{\Delta_T - \Delta_{CC}}{\Delta_{CC}} \times 100 \quad (1)$$

where Δ_T is the average surface strength at 28 days when one or two technologies were used, this is, SCC, CPF, SCC combined with CPF and Δ_{CC} is the average surface strength at 28 days for CC.

Table 4
Specific gravity and converted compressive strength of cores. Average results and variation coefficient in brackets.

Concrete property	Location	No. of cores	SCC	CC
Specific gravity (kg/m^3)	Wall A	6	2339 (1.3%)	2380 (2.0%)
	Wall B	6	2329 (1.2%)	2345 (2.8%)
	Slab	6	2305 (0.8%)	2289 (0.6%)
Compressive strength (MPa)	Wall A	6	67.9 (3.1%)	67.5 (2.2%)
	Wall B	6	69.7 (3.0%)	66.3 (6.0%)
	Slab	6	70.7 (7%)	58.1 (8.0%)

Table 5
Surface hardness of SCC and CC box-culvert walls. Median, average results and variation coefficient in brackets.

Reference	Age of concrete (days)	SCC		CC	
		$R_{s,\ median}$ (MPa)	$R_{s,\ average}$ (MPa)	$R_{s,\ median}$ (MPa)	$R_{s,\ average}$ (MPa)
Wall A, CPF-A face	7	36.0	36.0 (4.2%)	34.0	34.7 (6.3%)
	14	38.0	37.9 (4.5%)	37.0	37.3 (6.1%)
	28	47.5	47.6 (8.2%)	42.0	42.1 (7.8%)
Wall A, non-CPF face	7	33.0	32.8 (4.6%)	32.0	32.0 (5.0%)
	14	35.0	35.1 (5.9%)	34.0	34.2 (5.4%)
	28	42.0	41.7 (5.6%)	38.0	37.7 (5.8%)
Wall B, CPF-B face	7	36.0	35.4 (6.4%)	36.0	36.4 (4.1%)
	14	37.0	37.2 (4.8%)	38.0	37.6 (5.0%)
	28	42.0	42.1 (8.4%)	44.0	44.7 (11.0%)
Wall B, non-CPF face	7	33.5	33.4 (6.9%)	32.0	32.5 (5.2%)
	14	37.0	36.2 (6.2%)	34.0	34.5 (5.8%)
	28	40.0	41.1 (8.9%)	38.0	38.0 (5.1%)

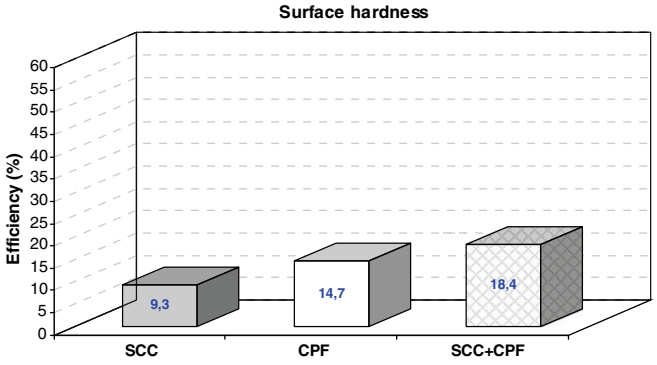

Fig. 7. Efficiency of SCC, CPF and SCC with CPF systems on surface hardness.

Results lead to the conclusion that surface hardness of CPF cast concrete is higher than for the same concrete cast traditionally. Comparing results from both box-culverts, surface hardness for SCC is higher than for CC and SCC combined with CPF is 18.4% more efficient than with CC. CPF-A is more efficient with SCC than with CC and CPF-B is more efficient with CC compared to SCC.

4.2. Durability properties

Durability of concrete largely depends on the ease with which fluids, both liquid and gases, can enter into, and move through pores of varying types and sizes of the concrete. The movement of the various fluids through concrete takes place not only by flow through the porous system, commonly referred to as permeability, but also by other mechanisms, diffusion and absorption [19]. When testing concrete for durability each mechanism is considered separately, but naturally, in real structures these mechanisms act together and in certain periods one or another may play a dominant role.

4.2.1. Water absorption by capillarity

Water absorption by capillarity was assessed following the procedure described in RILEM TC 166-PCD [20] slightly altered by suggestions in [21]. Cores 75 mm diameter were extracted from each side wall A and B of both box-culverts, from the CPF face right through to the non-CPF (control) face and 50 mm thick slices were sawn off from each end. These test-specimens were then put to dry in a ventilated heater at 40 °C until the difference between two consecutive weights was less than 0.5% of the original weight. For the test itself, cores were placed formwork face downwards, in a shallow water bath and supported on rods. Water level was adjusted so that the formwork face was dipped to a depth of approximately 3 mm. During the test, each test-specimen was weighed at time intervals up to 4.5 h from the start of the test. Similar tests conducted by other authors [7] have confirmed that absorption of water into concrete under capillary action is dependent on the square-root of time and may be modelled by the following Eq. (2), enabling determination of concrete sorptivity (S):

$$A = a_0 + St^{0.5} \tag{2}$$

where A (mg/mm^2) is the water absorption by unit area of concrete surface since the moment the core is dipped in water, t is the elapsed time and a_0 (mg/mm^2) is the water absorbed initially by pores in contact with water. Results of this test are presented in Tables 6 and 7, respectively, for core samples taken from the SCC box-culvert and CC box-culvert.

4.2.2. Resistance to chloride ion penetration

Resistance to chloride ion penetration was carried out using non-steady migration tests, ASTM C1202 [22] more popular in America and the more recent CTH Rapid Method (Chalmers University of Technology, Sweden) created by *Luping* and described in NT BUILD 492 [23]. This last method was adopted in Portugal through a LNEC specification, LNEC E 463 [24].

4.2.2.1. ASTM C1202 method. The ASTM C1202 method consists of monitoring the amount of electrical current passed through an

Table 6
Durability properties of cores from the SCC box-culvert. Average results and variation coefficient in brackets.

Concrete property	Location	No. of cores	Average (v.c.)
Water absorption by capillarity - Sorptivity ($g/(m^2 \times min^{1/2})$)	Wall A, CPF-A face	3	45.07 (4.8%)
	Wall A, non-CPF face	3	52.94 (10.2%)
	Wall B, CPF-B face	2	38.44 (–)
	Wall B, non-CPF face	3	46.84 (0.1%)
Resistance to chloride (ASTM C1202) - Electric charge (Coulombs)	Wall A, CPF-A face	4	2534 (4.6%)
	Wall A, non-CPF face	4	3068 (5.9%)
	Wall B, CPF-B face	4	2648 (3.3%)
	Wall B, non-CPF face	4	3191 (6.6%)
Resistance to chloride (CTH Rapid test) - D_{ns} (cm^2/s)	Wall A, CPF-A face	4	9.6×10^{-8} (6.9%)
	Wall A, non-CPF face	4	10.0×10^{-8} (23.0%)
	Wall B, CPF-B face	4	9.6×10^{-8} (8.8%)
	Wall B, non-CPF face	4	11.4×10^{-8} (9.9%)
Resistance to carbonation - d_k (mm)	Wall A, CPF-A face	3	4.0 (8.5%)
	Wall A, non-CPF face	3	6.8 (10.2%)
	Wall B, CPF-B face	2	5.0 (–)
	Wall B, non-CPF face	2	8.8 (–)

Table 7
Durability properties of cores from the CC box-culvert. Average results and variation coefficient in brackets.

Concrete property	Location	No. of cores	Average (v.c.)
Water absorption by capillarity - Sorptivity ($g/(m^2 \times min^{1/2})$)	Wall A, CPF-A face	3	69.60 (7.5%)
	Wall A, non-CPF face	3	76.04 (2.8%)
	Wall B, CPF-B face	2	60.73 (–)
	Wall B, non-CPF face	2	69.30 (–)
Resistance to chloride (ASTM C1202) - Electric charge (Coulombs)	Wall A, CPF-A face	3	3915 (6.4%)
	Wall A, non-CPF face	3	4218 (5.0%)
	Wall B, CPF-B face	4	3868 (8.8%)
	Wall B, non-CPF face	4	4384 (11.6%)
Resistance to chloride (CTH Rapid test) - D_{ns} (cm^2/s)	Wall A, CPF-A face	4	15.0×10^{-8} (4.3%)
	Wall A, non-CPF face	3	16.0×10^{-8} (20%)
	Wall B, CPF-B face	3	13.6×10^{-8} (5.4%)
	Wall B, non-CPF face	4	15.6×10^{-8} (4.7%)
Resistance to carbonation - d_k (mm)	Wall A, CPF-A face	–	–
	Wall A, non-CPF face	3	8.6 (7.5%)
	Wall B, CPF-B face	2	4.5 (–)
	Wall B, non-CPF face	2	10.0 (–)

approximately 100 mm diameter by 50 mm thick concrete specimen, when a potential difference of 60 V is maintained across the specimen for a period of 6 h. Chloride ions are forced to migrate out of a NaCl solution subjected to a negative charge through the concrete into a NaOH solution maintained at a positive potential. The conditioning of the concrete disc specimens for the test procedure consists of 1 h of air drying, 3 h of vacuum (pressure <600 mm Hg), 1 h of additional vacuum with specimens under deaerated water, followed by 18 h of soaking in water. The total charge passed, in coulombs, is used as an indicator of the resistance to the passage of chloride ions, the lower it is, the more resistant is the concrete to chloride penetration.

4.2.2.2. CTH rapid method. The CTH rapid method is based on a theoretical relationship between diffusion and migration which enables the calculation of the chloride diffusion coefficient. It is based on measuring the depth of colour change of a silver nitrate solution sprayed on specimens previously submitted to a migration test and application of the following equation:

$$D_{ns} = \frac{RT}{zFE}\frac{x_d - \alpha\sqrt{x_d}}{t} \quad (3)$$

where

$$E = \frac{U-2}{L} \quad (4)$$

$$\alpha = 2\sqrt{\frac{RT}{zFE}} \cdot erf^{-1}\left(1 - \frac{2C_d}{C_o}\right) \quad (5)$$

where D_{ns} is the apparent diffusion coefficient obtained in a non-steady-state migration test (cm^2/s); R the gas constant ($R = 8.314$ J/(mol K)); T the average value of the initial and final temperatures in the anolyte solution (K); L the thickness of the specimen (cm); z the absolute value of ion valence, for chloride, $z = 1$; F the Faraday constant ($F = 9.648 \times 10^4$ J/(V mol)); U the absolute value of the applied voltage (V); x_d the average depth of chloride penetration measured by using a colorimetric method (cm); t the test duration (s); C_d the concentration of free chloride at which the colour changes when using the colorimetric method to measure the chloride penetration depth ($kg_{Cl}/m^3_{solution}$); and C_o is the concentration of free chloride in the catholyte solution ($kg_{Cl}/m^3_{solution}$).

The procedure for determining the apparent diffusion coefficient (D_{ns}) consisted of after switching off the electrical field, the specimens were split in two halves and the penetration of chlorides was measured by using the colorimetric method. This method consists of spraying silver nitrate solution over the split faces, storing them in a dark place for an hour and then exposing them under a fluorescent light for a few hours, after which the average front of the white zone in the central part of each specimen is measured with a precision of 0.5 mm.

4.2.2.3. Results. Both methods were carried out on different specimens 50 mm thick sawn off the ends of 100 mm cores, drawn

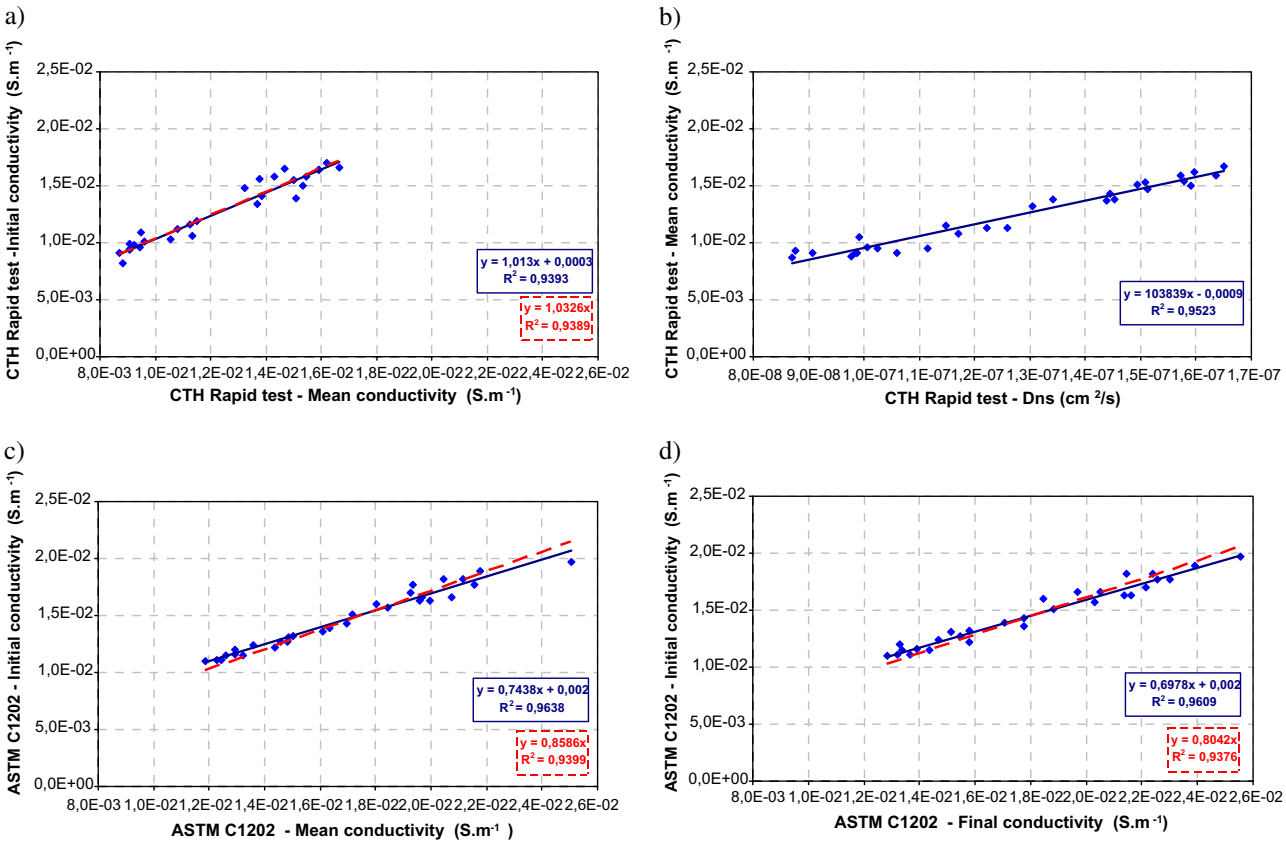

Fig. 8. Correlation between results of CTH Rapid test and ASTM C1202 test.

out from each side wall of both box-culverts. Results of ASTM C1202 test and CTH Rapid Test are presented in Tables 6 and 7, respectively, for different core samples taken from the SCC box-culvert and CC box-culvert.

The migration tests also enabled determining conductivity in saturated conditions, as the specimens must be fully saturated prior to testing. Therefore, when current is imposed during the test, conductivity (Eq. (6)) gives an indication on how easily electric current flows through the saturated pore system.

$$\sigma = \frac{1}{\rho} = \frac{1}{R} \cdot \frac{L}{A} = \frac{IL}{VA} \tag{6}$$

where σ is the conductivity ($S\ m^{-1}$), ρ the electric resistivity (Ω m), R the electric resistance (Ω), I the current (A), V the voltage (V), L the length (m), and A is the area of the test-specimen across which current passes (m^2). For initial conductivity determination, current I (A) was taken after 15 min of the beginning of the CTH Rapid Test and after 5 min of the beginning of the ASTM C1202 Test.

In fact, the electric current (I), measured in Amperes, is defined as the amount of electric charge (Q), measured in Coulombs, flowing through the cross-section of the test-specimen, over time (t), Eq. (7). Therefore, the total charge passed through a specimen, in coulombs, according to Eq. (6) and (7), enables determination of the mean conductivity of the specimen throughout the test

$$I = \frac{Q}{t} \tag{7}$$

Graphs a and c presented in Fig. 8 illustrate correlation between initial conductivity determined from initial electric current and mean conductivity calculated from the total charge passed throughout the test. This analysis made it possible to conclude that initial and mean conductivity are well correlated, concerning both tests, with R^2 of 0.94 and 0.96 for the CTH Rapid Test and the ASTM C1202 test, respectively. It was also possible to deduce that for the CTH Rapid Test initial and mean conductivity values are practically the same ($y = 1.0326x$) but for the ASTM C1202 test mean conductivity calculated from the total charge passed, is about 15% higher than initial conductivity ($y = 0.8586x$). Considering this last test, conductivity calculated from final electric current is approximately 20% higher than initial conductivity ($y = 0.8042x$), Fig. 8d. In fact, recently some doubts have been expressed with regard to this test. The main criticism is that the conditions of measurement are severe and may cause both physical and chemical change in the specimen, resulting in unrealistic values [25]. However the ASTM C1202 test is versatile and rapid to conduct and provides results that are easy to interpret.

For the CTH Rapid test also good correlation was found between mean conductivity and the diffusion coefficient ($R^2 = 0.95$), see Fig. 8b. According to the Nernst–Einstein equation, for a given concrete with a given moisture condition, there is a general relationship between chloride diffusivity and electrical resistivity or conductivity [26]. The Nernst–Einstein equation states:

$$D_i = \frac{RT\sigma t_i}{z_i^2 F^2 C_i} \tag{8}$$

where D_i is the diffusivity of species i, R is the gas constant, T is the absolute temperature, σ is the conductivity of concrete, z is the ion valence of species i, F is Faraday constant, C_i is the concentration of species i and t_i is the transference number of species i, which is defined as the proportion of current carried by this ion in relation to the current carried by the rest of the ions [27,28].

In fact, when the transference number of an ion is known, in this case a chloride ion, the diffusivity of this ion in concrete can be obtained by measuring the total conductivity of the concrete.

However, the calculation of the diffusion coefficient of the chloride ion, using conductivity measurements, does not take into account the reaction of chlorides with cement phases and therefore, the values obtained correspond to the effective diffusion coefficient (D_{eff}) and not to the apparent diffusion coefficient (D_{app}) [28,29]. On the other hand the transference number of chloride ions is difficult to measure because is complex to quantitatively describe the ionic components of the pore solution that participate in the migration process [30]. If these difficulties could be solved, in routine testing, the resistance against chloride penetration could more easily be monitored by testing the conductivity or electrical resistivity.

4.2.3. Resistance to carbonation

Resistance to carbonation was assessed in accordance with the procedure described in LNEC specification LNEC EE 391 [31] where specimens were exposed to 5 ± 0.1% carbon dioxide, relative humidity (RH) of 60 ± 5% and temperature of 23 ± 3 °C, in an accelerated carbonation chamber. Specimens used were sawn off the ends of 94 mm diameter cores extracted from the side walls of the box-culverts. Results of this test are also presented in Tables 6 and 7, respectively, for SCC and CC core samples. In the case of CPF-A with conventional concrete no results were obtained because specimens were damaged.

4.2.4. Discussion

Considering hardened SCC and conventional vibrated concrete of similar strength, it can be assumed that properties are comparable. Results of the durability-related properties considered presented in Tables 6 and 7 may be presented in terms of efficiency comparing effect of one or two technologies with the effect on CC, Fig. 9. Analysing these results makes it possible to, on one hand, compare performance of SCC, CPF-A and CPF-B versus CC in terms of durability and on the other hand, evaluate the efficiency of each CPF system, CPF-A and CPF-B on SCC comparing it with CC.

Concrete in the SCC box-culvert presented lower sorptivity, this is, absorption by capillarity, higher resistance to chlorides and to carbonation. Considering the first two parameters, SCC technology leads to a 30% enhancement whilst for carbonation resistance efficiency is around 16%. In theory, the factors controlling durability-related properties depend on the amount of paste, the pore structure and the interfacial aggregate/paste zone. Fresh SCC compared to CC is more stable and the extra powdered material used, together with the absence of vibration, leads to a more homogeneous microstructure with denser interfacial zones.

All tests carried out confirmed that durability-related parameters are improved with either CPF system. CPF-B, with a stiffer filter-drain compared to CPF-A, led to higher quality concrete cover in terms of absorption by capillarity (17.2%) and chloride ingress (approximately 12%). SCC technology seems more efficient for absorption by capillarity and resistance to chloride ingress whereas CPF reveals better performance in terms of resistance to carbonation.

Using SCC together with controlled permeability formwork leads to 40–50% enhancement of properties in the concrete cover. Comparing absorption by capillarity and chloride ion results, CPF on SCC presents similar efficiency to CPF on CC. However, in some cases, CPF on SCC proved to be more effective than on CC probably because of the extra powdered materials in the SCC which in the concrete cover, as a result of CPF, are drawn and retained at the concrete surface.

It should be mentioned that the comparison of the durability parameters were based on tests performed in specimens extracted from the box-culvert side walls, only. The slab, wherein the concrete compaction was less efficient in case of CC box-culvert (see Section 4.1.1), was not considered in the analysis, otherwise, the beneficial effect of SCC and CPF would be expected to be greater.

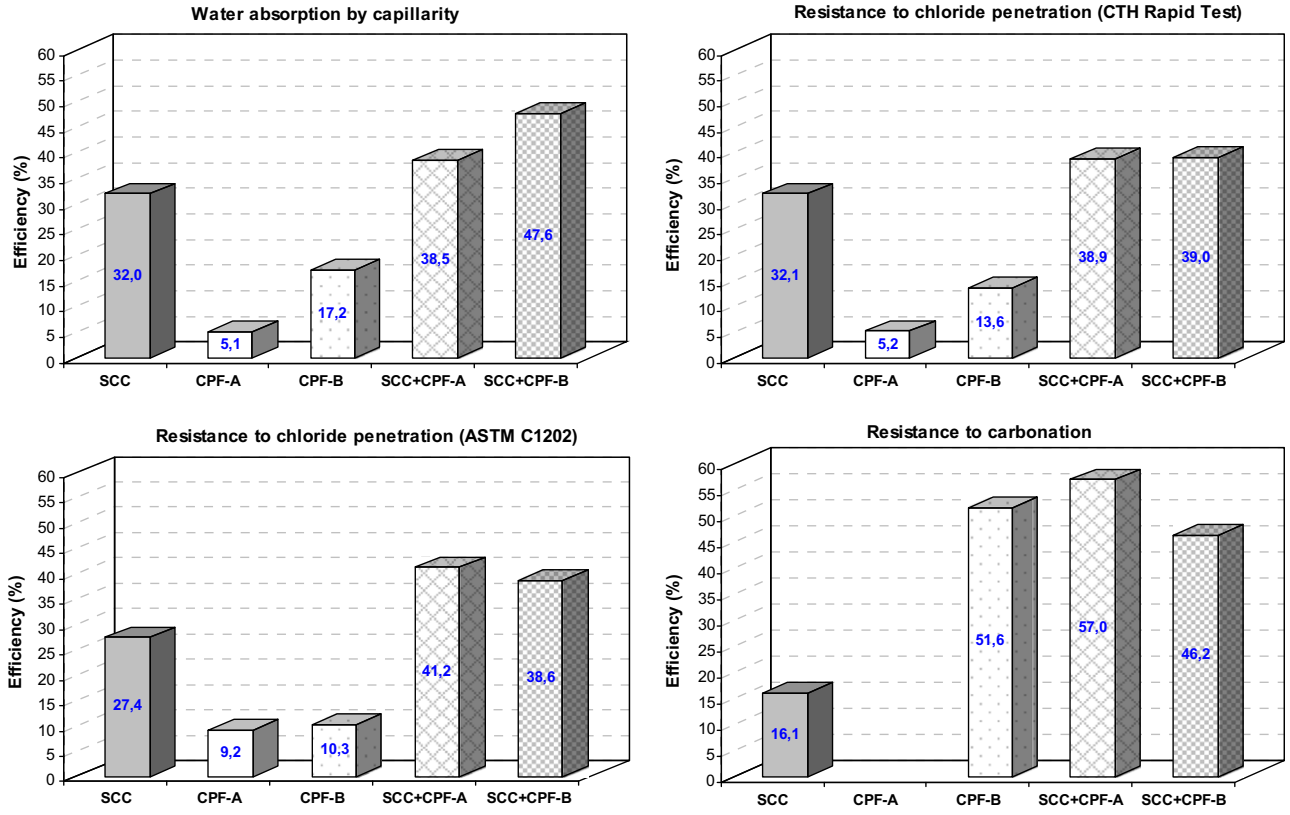

Fig. 9. Efficiency of SCC, CPF-A, CPF-B, SCC with CPF-A and SCC with CPF-B systems on durability properties.

5. Conclusions

Results obtained throughout the present research program carried out in actual on site conditions, led to the following conclusions:

- Innovative technologies such as SCC and CPF seem to be technically and economically viable when used on site.
- Using SCC compared to CC may lead to an overcost in materials of 18%, but final cost will be reduced due to energy and work savings related to absence of compaction as well as savings related to enhanced durability. In terms of CPF, costs may be reduced by suppression of releasing agents and of surface repairing. Overall costs will also be mitigated by reuse of certain CPF systems as well as enhanced durability.
- Tests carried out showed that SCC with adequate mix proportions, production process and casting is, in general, denser and more homogeneous compared to similar conventional concrete. Thus, using SCC enhances performance of concrete structures in terms of strength and durability.
- The concrete surfaces resulting from CPF were blow-hole free with no blemishes but the non-CPF faces, corresponding to the inner sides of the box-culverts side walls, presented the usual blow-holes which were more prolific in the CC compared to SCC.
- SCC and CPF enhance quality of the concrete cover as SCC is less vulnerable to penetration of water and aggressive agents. However, efficiency of CPF technology depends on the system used.
- Using both technologies together, controlled permeability formwork on SCC, durability-related parameters analysed improved 40–50%.
- Efficiency of CPF on SCC is similar to efficiency on CC, however, in some cases, CPF on SCC promotes a synergetic effect in terms of quality of the concrete cover thus contributing to sustainable construction.
- A more detailed analysis of the CTH Rapid test and ASTM C1202 results led to the conclusion that measuring initial electric conductivity or resistivity possibly consists of a rapid and economic way to predict resistance of concrete to chloride ion ingress. Further research work will be carried out on correlation between conductivity (σ) and apparent diffusion coefficient (D_{app}), involving more accurate assessment of the transference number values, t_i, in the Nernst–Einstein equation (see Eq. (8)).

Acknowledgements

The authors are deeply grateful to Agência de Inovação, S.A for financial support and to "Mota-Engil", "Sika", "Maprel", "Riobom Trading" and "Fibertex" for their collaboration as well as support from "Fundação para a Ciência e Tecnologia" sponsoring the PhD Grant for the first author (SFRH/BD/25552/2005) and also the Project POCTI/ECM/46820/2002.

References

[1] Sakai K, Shimonura T, Sugiyama, T. Design of concrete structures in the 21st century. Controlling concrete degradation. In: Dhir Ravindra, Moray D, editor. Proceedings of the international conference held at the University of Dundee, Newlands, Scotland, UK, 7 September 1999.
[2] Shah SP, Akkaya Y, Bui VK. Innovations in microstructure, processing and properties. Innovations and Developments in concrete Materials and Construction. In: Dhir Ravindra, Hewlett Peter C, Csetenyi Laszlo J, editor. Proceedings of the international conference held at the University of Dundee, Scotland, UK, 9–11 September 1999.
[3] Swamy RN. Sustainable concrete for the 21st Century. Concept of strength through durability. Indian Concrete J 2007;81(December):7–15.
[4] Okamura H, Ozawa K, Ouchi M. Self-compacting concrete. Struct Concrete J fib 2000;1(1):3–17.
[5] Skarendahl A, Petersson O. Self-compacting concrete. State-of-the-art report of RILEM Committee 174-SCC. Report 23. RILEM Publications; 2001. p. 154.
[6] EFNARC, The European Guidelines for Self-Compacting Concrete, May 2005. <www.efnarc.org>.
[7] Coutinho J. The combined benefits of CPF and RHA in improving the durability of concrete structures. Cement Concrete Compos 2003.
[8] EN 1097-6:2000. Tests for mechanical and physical properties of aggregates. Determination of particle density and water absorption; 2000.
[9] Walraven J. Self-compacting concrete: challenge for designer and researcher. In: Shah SP, editor. Proceedings of the second North American conference on the design and use of self-consolidating concrete and the fourth international RILEM symposium on self-compacting concrete. Chicago, United States of America; 2005. p. 431–45.
[10] Nunes S. Experimental study and numerical modelling of self-compacting concrete. In: Walraven J, Blaauwendraad J, Scarpas T, Snidjer B, editors. Proceedings of the 5th international PhD symposium in Civil Engineering, Delft, The Netherlands; 2004. p. 857–65.
[11] Nunes S, Figueiras H, Sousa Coutinho J, Figueiras J. Método para definição da composição de betão auto-compactável Self-compacting concrete mix-design method. E-Mat-Revista de Ciência e Tecnologia de Materiais de construção Civil 2005;2(1):1–11.
[12] Klug Y, Holschemacher K. Comparison of the harden properties of self-compacting and normal vibrated concrete. In: 3rd international RILEM symposium on self-compacting concrete, Reykjavik, Iceland, 17–20 August, 2003.
[13] Nunes S, Figueiras H, Coutinho J, Figueiras J. SCC and conventional concrete site: property assessment. RIEM – Revista IBRACON de Estruturas e Materiais. (accepted for publication).
[14] Juvas K. Experiences with SCC in the production of prefabricated elements. In: Wallevik O, Nielsson I, editors. Proceedings of the 3rd international RILEM symposium, Reykjavik, Iceland; 2003.
[15] Coutinho J. Melhoria da durabilidade dos betões por tratamento em cofragem. PhD, Engenharia Civil, Faculdade de Engenharia da Universidade do Porto. Publicado pela FEUP edições em 2005. ISBN223433/05.
[16] Price WF. Controlled permeability formwork. CIRIA Report C511; 2000.
[17] Mansur MA, ASCE M, Islam MM. Interpretation of concrete strength for non-standard specimens. J Mater Civil Eng 2002:151–5.
[18] EN 12504-2:2001. Testing concrete in structures. Non-destructive testing. Determination of rebound number; 2001.
[19] Neville AM. Properties of concrete. England: Longman; 1998.
[20] RILEM TC116-PCD. Permeability of concrete as a criterion of its durability, C: determination of the capillary absorption of water of hardened concrete. Mater Struct 1999;32:178–9.
[21] Sonebi M, Bartos PJM., Zhu W, Gibbs J, Tamini A. Final Report of Task4: properties of hardened concrete, rational production and improved working environment trough using self compacting concrete. Brite Euram Project BRPR-CT96-0366, <http://scc.ce.luth.se>, 15-08-2001 10:30.
[22] ASTM C1202. Standard test method for electrical indication of concrete's ability to resist chloride ion penetration. American Society for Testing Materials; 1997.
[23] NT BUILD 492. Concrete, mortar and cement-based materials: Chloride migration coefficient from non-steady-state migration experiments. NORDTEST; 1999.
[24] Especificação LNEC E 463. BETÃO. Determinação do coeficiente de difusão dos cloretos por ensaio de migração em regime não estacionário; 2004.
[25] Feldman R, Prudencio L, Chan G. Rapid chloride permeability test on blended cement and other concretes: correlations between charge, initial current and conductivity. Constr Build Mater 1999;13:149–54.
[26] Gjørv OE. Durability design and construction quality of concrete structures. In: Yuan Y, Shah P Lu H, editors. Proceedings of the international conference in advances in concrete and structures, Rilem Publications; 2003. p. 309–19.
[27] Lu X. Application of the Nernst–Einstein equation to concrete. Cement Concrete Res 1997;27(2):293–302.
[28] Andrade C. Calculation of chloride diffusion coefficients in concrete from ionic migration measurements. Cement Concrete Res 1993;23:724–42.
[29] Andrade C, Rio O, Castillo A, Castellote M, Andrea R. A NDT performance method based on electrical resistivity for the specification of concrete durability. In: Eberhardsteiner J, et al., editors. Proceedings of the thematic conference on computational methods in tunnelling, Vienna, Austria: 2007.
[30] Gjorv OE, Zhang T. Migration testing of chloride diffusivity in concrete. In: Gjorv OE, Sakai K, Banthia N, editors. Proceedings of the 2nd international conference on concrete under sever conditions – environment and loading, Tromso, Norway; 1998.
[31] Especificação LNEC E 391. Determinação da resistência à carbonatação; 1993.